Available online at www.sciencedirect.com
SCIENCE DIRECT®
Biochemical and Biophysical Research Communications 331 (2005) 1099–1106
BBRC
www.elsevier.com/locate/ybbrc

Molecular cloning and characterization of the murine gnathodiaphyseal dysplasia gene *GDD1*

Satoshi Tsutsumi [a], Hiroshi Inoue [a,*], Yukiko Sakamoto [a], Kuniko Mizuta [b], Nobuyuki Kamata [b], Mitsuo Itakura [a]

[a] *Division of Genetic Information, Institute for Genome Research, The University of Tokushima, Tokushima, Japan*
[b] *Department of Oral and Maxillofacial Surgery, Division of Cervico-Gnathostomatology, Hiroshima University Graduate School of Biomedical Sciences, Hiroshima, Japan*

Received 28 March 2005
Available online 11 April 2005

Abstract

Mutations in the *GDD1* gene cause gnathodiaphyseal dysplasia, a rare human skeletal syndrome with autosomal dominant inheritance. The biochemical function(s) of GDD1 protein and the molecular pathophysiology of *GDD1* mutations leading to GDD have not yet been elucidated. In this study, we characterized the complete cDNA sequence and genomic organization of the mouse *GDD1* gene. Analysis of *GDD1* mRNA revealed a complex alternative splicing pattern, involving five exons of the *GDD1* gene. GDD1 isoforms lacking conserved amino acids at the N-terminus cytoplasmic tails, and with changes in transmembrane topology, are presumably associated with changes in protein functions and subcellular localizations of GDD1. We found *GDD1* expression to be up-regulated during the course of myogenic differentiation in the murine pluripotent mesenchymal precursor cell line C2C12, whereas its expression was diminished during osteoblastic differentiation. These observations suggest diverse cellular roles of GDD1 protein.

Keywords: GDD1; Gnathodiaphyseal dysplasia; TMEM16 gene family; Myogenesis; Osteogenesis

Gnathodiaphyseal dysplasia (GDD; MIM 166260), a rare autosomal dominant skeletal syndrome, is characterized by bone fragility, gross thickening of the diaphyseal cortices of long bones, generalized osteopenia affecting other bones, and cemento-osseous lesions of the jawbones [1,2]. GDD patients begin to experience frequent bone fractures around puberty and are susceptible to purulent osteomyelitis in jawbones during adult life. Since Akasaka et al. [1] first described a Japanese family with GDD in 1969, phenotypically similar families with different ethnic backgrounds have also been documented [3,4]. Studying the Japanese family reported by Akasaka et al., we previously mapped the GDD disease locus to chromosome 11p14.3–15.1 [5]. Subsequently, employing a positional cloning approach to examine this chromosome region, we identified a novel gene responsible for GDD and gave it the name *GDD1* (*gnathodiaphyseal dysplasia 1*) [6]. Screening for the *GDD1* gene in this Japanese family revealed all affected members to carry the heterozygous mutation of Cys356Arg caused by a T-to-C transition in exon 11. A different missense mutation in the same codon (Cys356Gly) was found in two affected members of another family of African-American origin [6].

The biochemical functions of GDD1 protein and molecular pathophysiology of *GDD1* mutations leading to GDD are as yet totally unknown. In human and murine tissues, the *GDD1* gene shows abundant expression in skeletal muscle and bone tissues including the

* Corresponding author. Fax: +81 88 633 9484.
E-mail address: hinoue@genome.tokushima-u.ac.jp (H. Inoue).

0006-291X/$ - see front matter © 2005 Elsevier Inc. All rights reserved.
doi:10.1016/j.bbrc.2005.03.226

calvarium, femur, and mandible [6]. Secondary structure analysis suggested that the gene encodes a 913 amino acid integral membrane protein with eight membrane-spanning domains. Preliminary immunofluorescence localization of the epitope-tagged GDD1 protein in cultured cells revealed an endoplasmic reticulum (ER) localization, indicating possible GDD1 protein involvement in the regulation of Ca^{2+} homeostasis, the folding, oligomerization, and glycosylation of proteins, and the formation and isomerization of disulfide bonds within proteins. Along with the GDD disease phenotype, these findings suggest GDD1 to play a key and novel role in muscle/skeletal development and metabolism.

Interestingly, *GDD1* was found to be a member of the novel TMEM16 gene family [7–11], which was recently identified on the basis of sequence conservation within the human genome and similarity in computational secondary protein structure. Members of this gene family have a common structural topology with eight-transmembrane domains and a unique sequence motif called the annotated domain of unknown function 590 (DUF590). Although members of the TMEM16 family including GDD1 are expected to have, at a minimum, similar biochemical functions and cellular localization, only very limited information is available at present [12].

In this study, to provide a foundation for further functional and genetic studies of GDD1, we characterized the mouse *GDD1* gene. Mouse *GDD1* showed unique expression patterns in tissues, with multiple alternative splicing events. *GDD1* expression was up-regulated during in vitro myogenic cell differentiation. In addition, a comprehensive expression analysis of the human *GDD1*-related TMEM16 gene family was undertaken in various human tissues and cell lines to identify the unique expression patterns of these genes.

Materials and methods

Isolation of total RNAs from tissues and cultured cells. All animal experiments were conducted under protocols approved by the IACUC Committee of the University of Tokushima. Total RNA was extracted from the brain, heart, lung, liver, kidney, skeletal muscle, and calvarial bones of 3-week-old BDF1 mice (CLEA Japan, Japan) using ISOGEN reagent (Nippon Gene, Japan) following the manufacturer's protocol. The C2C12 mouse myoblast cell line (CRL-1772) was obtained from the RIKEN Cell Bank (Tsukuba, Japan) and cultured in growth medium (GM) containing high-glucose DMEM (Invitrogen, Japan) supplemented with 15% fetal bovine serum (FBS) and antibiotics (100 U/ml penicillin-G, 100 μg/ml streptomycin) at 37 °C in a humidified incubator under 5% CO_2. Total RNA from C2C12 cells was extracted using ISOGEN reagent.

3′ rapid amplification of cDNA ends (3′RACE) analysis and reverse-transcription polymerase chain reaction amplification. A 3′RACE analysis of mouse *GDD1* mRNA was performed using mouse skeletal muscle total RNA with the GeneRacer kit (Invitrogen), following the manufacturer's protocol. Mouse *GDD1* EST sequences were searched for using the University of California Santa Cruz (UCSC) genome browser (http://genome.ucsc.edu). To amplify the 3′-untranslated region of *GDD1*, a reverse PCR primer of AK-R (5′-CTA TTG AGG TCA ATA ACT GAA GAC AC-3′) was designed within EST AK035179 and used for reverse-transcription polymerase chain reaction (RT-PCR) with a forward primer of GDD1-F (5′-AAA TCA TAG CAG CAG TGC ATC -3′) located within the coding sequence of GDD1. For RT-PCR, first strand complementary DNA (cDNA) was synthesized from 2 μg of total RNA using random hexamers and Superscript III reverse transcriptase (Invitrogen). Oligonucleotides were obtained from the Hokkaido System Science (Sapporo, Japan). The RT-PCR was performed using KOD-Plus DNA polymerase (Toyobo, Japan) under the following conditions: 94 °C for 2 min, followed by 35 cycles at 94 °C for 15 s, 55 °C for 30 s, and 68 °C for 4 min. The PCR product was subcloned into a pCR2.1-TOPO vector (Invitrogen) and sequenced using the ABI Prism Big Dye Terminator Cycle Sequencing system (Applied Biosystems, Japan) on an ABI PRISM 3100 Genetic Analyzer (Applied Biosystems). Gene structure and the exon–intron boundaries were determined by comparing the cDNA sequence with the mouse genomic sequence available through the UCSC genome browser (UCSC Genome Assembly, May 2004).

Northern blot analysis. Ten microgram total RNAs from mouse tissues was separated on a 1% agarose–formaldehyde gel and blotted onto a Hybond XL nylon membrane (Amersham Biosciences, USA). A DynaMarker RNA High (0.2–9.0 kb, BioDynamics Laboratory, Japan) was run in parallel as a size marker. A 2.8-kb cDNA fragment corresponding to the full coding sequence of mouse *GDD1* (nucleotides 151–2974 of GenBank Accession No. AB125740) was amplified by RT-PCR using KOD-Plus DNA polymerase (Toyobo), and was labeled with ^{32}P using a Random Primer DNA Labeling Kit Ver.2 (Takara, Japan). Hybridization was performed at 65 °C overnight with the labeled probe in Church buffer, consisting of 0.2 M Na_2HPO_4, pH 7.2, 7% SDS, and 1 mM EDTA. After hybridization, the membrane was washed twice in 2× SSC with 0.1% SDS at 65 °C for 30 min and twice in 0.2× SSC with 0.1% SDS at 65 °C for 30 min, and was exposed at −80 °C to BioMax X-ray film (Eastman Kodak Co.) with an intensifying screen for 24 h. A mouse glyceraldehyde phosphate dehydrogenase (GAPDH) probe was used to confirm RNA integrity.

Identification of alternative splicing variants. To amplify the complete coding sequence of mouse *GDD1*, PCR primers CDS-F (5′-GGT CCT TCA ATG CCT TCA ACG AG-3′) and CDS-R (5′- AGA GGC AAC AGT GGA TAG AG-3′) were designed within exons 1 and 22, respectively. PCR was performed with mouse skeletal muscle and brain cDNAs using KOD-Plus DNA polymerase (Toyobo). A ~2.8 kb PCR fragment was gel-purified, subcloned into a pCR2.1-TOPO vector (Invitrogen), and sequenced. To detect alternatively spliced *GDD1* exons separately, PCR primers were designed as follows: alternative exon 4, ex3F (5′-CTC ATC CCT GAA GAC TTA CAG-3′) and ex5R (5′-CCA CGT AGG ACA GGA CAA A-3′); alternative exon 6, ex5F (5′-TCG ACT TTG TCC TGT CCT AC-3′) and ex7R (5′-ACT TCA GCG TAA GTG ACC AG-3′); alternative exon 16 (Ex16b), ex15F (5′-AAG ATA TCT GCC TGG ATT ACG-3′) and ex17R (5′-AAT GAT GGT TAG CTG GGT GG-3′); alternative exons 20 and 21, ex19F (5′-CAT GGG AAT CCG AGT GGA TG-3′) and ex22R (5′-AAA ATT TAA ACA GAA ACA CGA CG-3′); and exons 13 and 14 (non-alternatively spliced exons); ex12F (5′-GAC TGT GTT CTT TGC GCT CTT-3′) and ex15R (5′-GAC TGA CAG GCG GTA TAT GA-3′). PCR was performed using Platinum *Taq* DNA polymerase (Invitrogen) under the following conditions: 94 °C for 2 min, followed by 30 or 35 cycles at 94 °C for 30 s, 55 °C for 30 s, and 72 °C for 30 s. To ensure the integrity of cDNA, mouse GAPDH was amplified with a primer pair of mGAPDH-F (5′-TGG TGA AGG TCG GTG TGA AC-3′) and mGAPDH -R (5′-TCA ATG AAG GGG TCG TTG ATG-3′). A commercial DNA size marker (1 kb Plus DNA Ladder, Invitrogen) and PCR products were separated on a 2% agarose gel containing ethidium bromide and imaged with a Printgraph AE-6911CX system (ATTO, Tokyo, Japan).

Induction of cell differentiation. Prior to the experimental treatments, C2C12 cells were inoculated into 35 mm culture dishes

(SUMILON, Japan) at a density of 3×10^4 cells/cm^2 and cultured overnight. For myogenic differentiation, GM was replaced with low-serum differentiation medium (Myogenic DM) consisting of DMEM and 2% horse serum. Differentiation of C2C12 cells into osteoblasts was achieved by incubation in osteoblastic DM: DMEM containing 2.5% FBS and 300 ng/ml of recombinant human bone morphogenetic protein (rhBMP)-2 (generously provided by Yamanouchi Pharmaceutical, Japan). After induction of cell differentiation, C2C12 cells were harvested at different time points (0, 6, 12, 24, 48, and 72 h) to extract total RNAs. The extents of myogenic and osteogenic inductions were verified by the expression of lineage specific marker genes, troponin T (TnT) and osteocalcin (OC), respectively. The PCR primers were as follows: mTnT-F (5′-AGA GCT CAT TGC ACT AAA AGA C-3′) and mTnT-R (5′-CTC TTC TTT GCC TCC TCC TC-3′); mOC-F (5′-CCC TGA GTC TGA CAA AGC CTT C-3′) and mOC-R (5′-TCA CAA GCA GGG TTA AGC TCA C -3′). To detect *GDD1* expression, primers of mGDD1-F (5′-CAT GGG AAT CCG AGT GGA TG -3′) and mGDD1-R (5′- GTG GAA TTC GTT GAG TAG GC-3′) were used. RT-PCR was performed using Platinum *Taq* DNA polymerase (Invitrogen) under the following conditions: 94 °C for 2 min, followed by 23 or 30 cycles at 94 °C for 30 s, 60 °C for 30 s, and 72 °C for 30 s.

Quantitative real-time RT-PCR analysis. Expressions of members of the TMEM16 family were analyzed using a 5′ nuclease (TaqMan) assay, with an ABI PRISM 7900HT Sequence Detection System (Applied Biosystems, Japan). Pre-developed TaqMan probes and primer sets for the human TMEM16 genes were obtained from Applied Biosystems and their assay IDs were as follows: ORAOV2 (TMEM16A); Hs00216121_m1, TMEM16B; Hs00220570_m1, TMEM16C; Hs00230040_m1, TMEM16D; Hs00400770_m1, GDD1 (TMEM16E, LOC203859); Hs01381120_g1, DKFZp313M0720 (TMEM16F); Hs01374899_m1, TP53I5 (PIG5); Hs00413380_g1, PCANAP5 (NGEP); and Hs00330215_m1. Expression levels of each TMEM16 gene were normalized using the level of *β-actin* expression as a reference (Human *β-actin*, Applied Biosystems, Cat. No. 4310881E). Human total RNAs were obtained from commercial sources: Human Total RNA Master Panel II (BD Biosciences, Cat. No. K4008-1) and the Human Cell Line MTC Panel (BD Biosciences, Cat. No. K1431-1). Universal Human Reference Total RNA (BD Biosciences) was made by pooling of the total RNAs from a collection of various tissues, which provided a good standardization of gene expression profiles. First strand cDNA was synthesized from 2 μg of total RNA using the Superscript III First-Strand Synthesis System (Invitrogen). Two nanograms of cDNA template was combined with 1X TaqMan Universal PCR MasterMix (without AmpErase UNG, Applied Biosystems), 200 nM of forward and reverse primers, and 250 nM probe. PCR was performed in triplicate in a MicroAmp optical 384-well plate in a total volume of 20 μl, using an ABI PRISM 7900HT Sequence Detection System. The cycle conditions were: 95 °C for 10 min, followed by 40 cycles at 95 °C for 15 s, 60 °C for 1 min. Data were collected with instrument spectral compensations using the Applied Biosystems SDS 2.1 software and analyzed by the threshold cycle (C_t) relative quantification method (Applied Biosystems). For data presentation, pseudocolor images were constructed using the Gradient Contour Chart, an Excel add-in software (Fig. 4).

Results and discussion

cDNA sequence and genomic structure of the mouse GDD1 gene

Development of appropriate animal models is anticipated to greatly facilitate elucidation of the functions of GDD1 protein responsible for the disease phenotype. We therefore endeavored to generate *GDD1* knockout mice based on micromanipulation of engineered ES cells. This required detailed information on cDNA, genomic structure, and expression of the mouse *GDD1* gene. As a first step, we characterized the mouse full-length *GDD1* cDNA. The 5′ end of the mouse *GDD1* transcript was previously characterized by 5′ RACE and RT-PCR analyses [6]. To isolate the 3′ end of the mouse *GDD1* transcript, we performed 3′ RACE analysis but failed to identify a *GDD1* transcript, presumably due to a large 3′-untranslated sequence (data not shown). We next searched the EST database (dbEST) with a ~10 kb

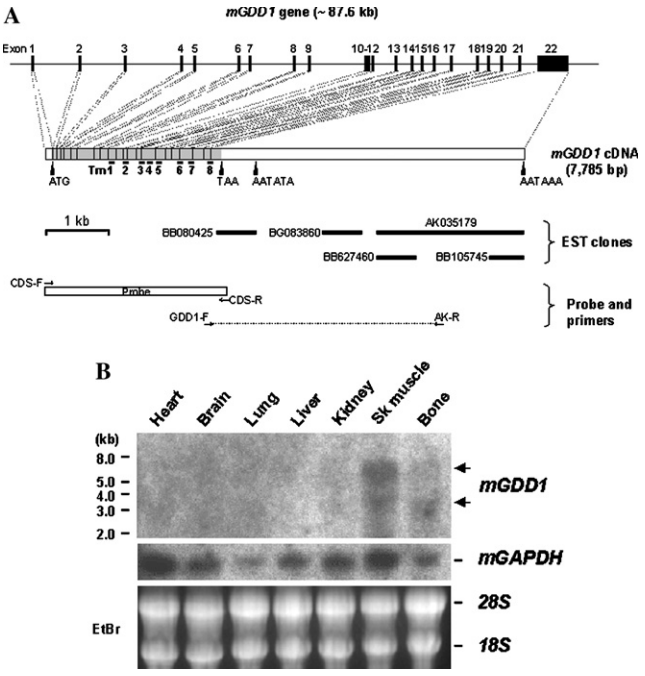

Fig. 1. Characterization of full-length cDNA and expression analysis of the mouse *GDD1*. (A) Schematic representation of mouse cDNA. The coding region (nt 207–2922, GenBank Accession No. AB206762) is shown in gray. The locations of the translation start codon (ATG), stop codon (TAA), and putative poly(A) adenylation signal sequences (classical; AATAAA, non-classical; AATATA) are indicated by solid triangles. Sequences coding putative transmembrane domains are shown as Tm1-8. The five EST clones (BB080425, BG083860, BB627460, AK035179, and BB105745) corresponding to the *GDD1* 3′ UTR sequence are shown as thick black bars. The exon structure was deduced by comparing the cDNA sequence to the genome sequences and is shown in the upper portion. The *GDD1* probe used for Northern blot and primers for RT-PCR analyses are shown in the lower portion. (B) Northern blot analysis of *GDD1* gene expression. Ten micrograms of total RNAs from mouse tissues was separated on a 1% agarose–formaldehyde gel followed by transfer to a nylon membrane and hybridization with a ^{32}P-labeled *GDD1* probe. Size markers in kilobases (kb) are shown on the left. Two different *GDD1* transcripts in sizes (7.8 and 3.5 kb) were observed in skeletal muscle and bone (arrows). The 7.8 kb transcript predominated in skeletal muscle and corresponded well with the predicted *GDD1* transcript size. The blot was rehybridized with labeled glyceraldehyde phosphate dehydrogenase (GAPDH) cDNA (middle). Levels of RNA loaded into each lane were assessed by the signal from the ethidium bromide (EtBr) stained 28S and 18S ribosomal RNAs (lower).

genomic sequence containing the 3′ end and the downstream portion of the *GDD1* coding sequence. This identified five ESTs: BB080425, BG083860, BB627460, AK035179, and BB105745 (Fig. 1A). Among these, an EST clone, AK035179, was 2413 bp in length and originated from the mouse embryonic body between the diaphragm region and neck. From this EST sequence, we designed the reverse primer AK-R and used it for RT-PCR analysis along with the forward primer, GDD1-F, located within the *GDD1* coding sequence. A 3.5 kb fragment was successfully amplified with mouse skeletal muscle cDNA, indicating AK035179 to be a part of the *GDD1* transcript. AK035179 contained a classical poly(A) adenylation signal sequence (AATAAA) at its end. Taking

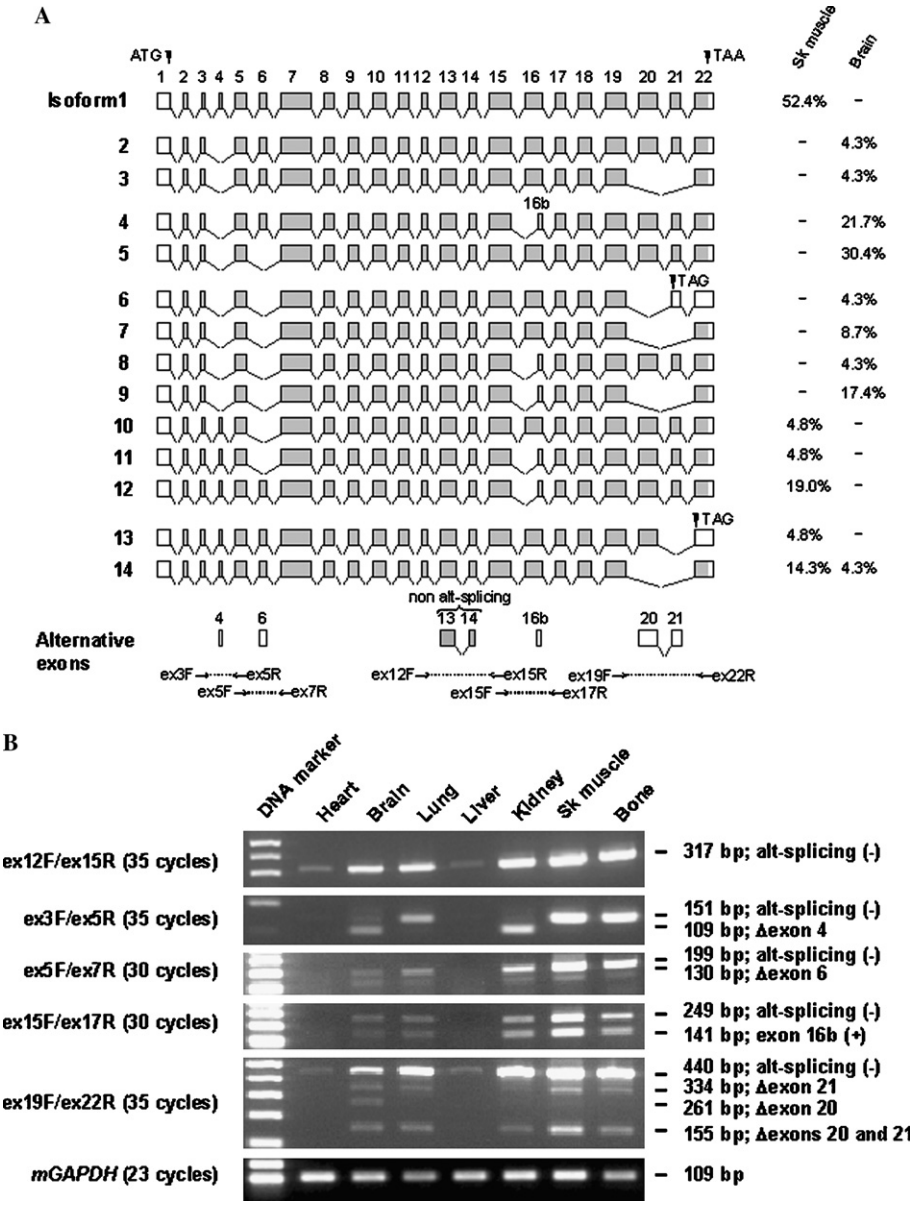

Fig. 2. Complex alternative splicing and exon usage of mouse *GDD1*. (A) Schematic representation of alternatively spliced *GDD1* isoforms. The entire coding sequence of mouse *GDD1* was amplified by PCR using cDNAs from skeletal muscle and brain tissue as templates. Products were subcloned into a pCR2.1-TOPO vector and ~24 clones each of skeletal muscle and brain tissue were sequenced. I-1 is the longest *GDD1* transcript containing all 22 exon sequences. Alternatively spliced *GDD1* isoforms (I-2 to I-14) are comprised of different combinations of alternative exons of 4, 6, 16b, 20, and 21. The translation start codon (ATG) and stop codons (TAA, TAG) are indicated by solid triangles. Frequencies (%) of the appearance of each isoform are shown on the right (Sk muscle: skeletal muscle, $n = 21$; brain, $n = 23$). Locations of primers for analyzing alternative exon usage (B) are shown below: exon 4, ex3F and ex5R; exon 6, ex5F and ex 7R; exon 16, ex15F and ex 17R; and exons 20 and 21, ex19F and ex22R; non-alternatively spliced exons 13 and 14 (positive control), ex12F and ex15R. (B) Analysis of alternative *GDD1* exon usage. Mouse total RNA was extracted from the brain, heart, lung, liver, kidney, skeletal muscle, and calvarial bone, and used for RT-PCR analysis. Primer pairs are shown on the left with numbers of PCR cycles (indicated in parentheses). Note that exons 13 and 14, non-alternatively spliced exons, are regarded as controls (top, primers ex12F and ex15R). mGAPDH; mouse glyceraldehyde phosphate dehydrogenase (cDNA control).

these results together, the size of the longest transcript of mouse *GDD1* was predicted to be 7785 bp (GenBank Accession No. AB206762), including a 5′-untranslated region of 206 bp, an ORF of 2715 bp (nt 207–2922), and a 3′-untranslated region of 4864 bp with a poly(A) adenylation signal 13 bp upstream from the poly(A) tail (Fig. 1A).

Alignment of the *GDD1* cDNA sequence with the mouse genomic sequence (UCSC Genome Assembly, May 2004) revealed the mouse *GDD1* gene to have a genomic organization similar to that of the human gene. Twenty-two exons were distributed over the 87.6 kb genomic region on chromosome 7 band B3 (Fig. 1A), a site previously established as having synteny with the human 11p14.3 region (data not shown). This observation indicates that human and mouse *GDD1* genes are localized in a region with conserved linkage homology. As in the human gene, there were no non-coding exons at the 5′ and 3′ ends, and the initiation and stop codons (ATG and TAA) were located within exons 1 and 22, respectively.

Northern blot analysis using the full coding sequence fragment as a probe showed high *GDD1* expression in skeletal muscle and bone tissues, confirming our previous observations (Fig. 1B). A 7.8 kb band (transcript) predominated in skeletal muscle and corresponded well with our prediction of transcript size. Mainly a 3.5 kb band was seen in bone. This band was also observed in skeletal muscle. The exact nature of this 3.5 kb band is unknown, but, since a non-classical polyadenylation signal sequence (AATATA) was located 4.3 kb upstream from the 3′ end, we speculate that this is attributable to either alternative polyadenylation of the transcript or to an unknown alternative splicing event in the 3′-untranslated region. In contrast to our previous Northern blot results obtained using human poly(A) RNAs [6], there was no detectable mouse *GDD1* signal in cardiac tissue.

Alternative splicing isoforms of mouse GDD1 mRNA

To search for the transcript variants within the coding sequence, long-range PCR was performed using cDNAs from skeletal muscle and brain tissue as templates. Primers CDS-F and CDS-R were chosen within exons 1 and 22 of the mouse *GDD1* gene (Fig. 1A), respectively, to amplify the entire coding sequence as one fragment. RT-PCR products were subsequently subcloned and ~24 clones each of skeletal muscle and brain origin were sequenced. Results showed a complex alternative splicing pattern generating 14 *GDD1* isoforms (I-1–I-14, for schematic representation see Fig. 2A). Five exons of the *GDD1* gene were involved in this alternative splicing (exons 4, 6, 16, 20, and 21): I-1, wild type containing all 22 exon sequences; I-2, exon 4 skipped; I-3, exons 4, 20, and 21 skipped; I-4, exon 4 skipped plus an alternative splicing acceptor site within exon 16 (exon 16b); I-5, exons 4 and 6 skipped; I-6, exons 4, 6, and 20 skipped; I-7, exons 4, 6, 20, and 21 skipped; I-8, exons 4 and 6 skipped plus use of exon 16b; I-9, exons 4, 6, 20, and 21 skipped plus use of exon 16b; I-10, of exon 6 skipped; I-11, exon 6 skipped plus use of exon 16b; I-12, use of exon 16b: I-13, exon 21 skipped; and I-14, exons 20 and 21 skipped. Skipping exons 4 (I-2–I-9) and 6 (I-5–I-11) produced in-frame deletions 14 (aa 39–52, GenBank Accession no. AB206762) and 23 (aa 91–113) conserved amino acids at the N-terminus cytoplasmic tails, respectively. Skipping exons 4 and 6 were frequently observed with cDNA clones from brain tissue (22/23 and 12/23 clones, respectively). Of note, multiple *GDD1* splice isoforms associated with changes in transmembrane topology were identified. The use of an alternative splicing acceptor site within exon 16 (exon 16b, I-4, I-8, I-9, I-11, and I-12) caused an in-frame deletion of 36 amino acids (aa 535–570) that included the entire putative transmembrane domain 5 (TM5). Skipping exon 20 (I-6) and exon 21 (I-13) resulted in frameshifts at aa 737 and 796, respectively, resulting in removal of TM7-8 regions and creation of a new termination codon (TAG) that caused the C-terminus end to be truncated. Deletion of both exons 20 and 21 (I-2, I-7, I-9, and I-14) resulted in an in-frame deletion of 95 amino acids (aa 737–831) between the TM7 and TM8 regions. These alternative splicing events and exon usage were also confirmed in tissues other than skeletal muscle and the brain by RT-PCR (Fig. 2B). Further investigation will be needed however, and we speculate that these multiple *GDD1* isoforms, especially isoforms with changes in transmembrane topology, may be associated with diverse cellular roles of GDD1 protein arising from alternations in functions or subcellular localizations.

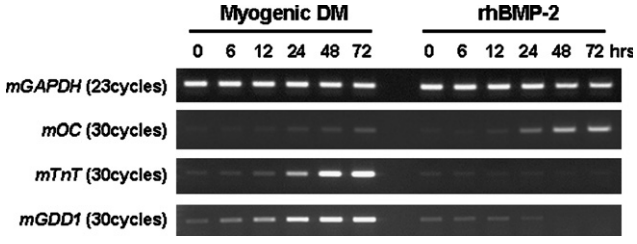

Fig. 3. *GDD1* gene expression during myogenic and osteoblastic differentiation. C2C12 cells were cultured in myogenic differentiation medium (myogenic DM) or treated with recombinant human BMP-2 (300 ng/ml) for the indicated time periods (0, 6, 12, 24, 48, and 72 h). Total cellular RNAs were extracted and used for RT-PCR. For each gene, the number of PCR cycles (indicated in parentheses) was optimized to achieve linear phase amplification. *GDD1* expression was up-regulated during myogenic differentiation in parallel with that of troponin T (TnT), a specific myogenic marker gene. Note that weak expression of osteocalcin (OC), a specific osteoblastic marker gene, was detectable 24 h after myogenic induction. Similar observations were made by another group [14]. Treatment with BMP-2 resulted in decreased expression of *GDD1*, while OC expression increased markedly. mGAPDH; mouse glyceraldehyde phosphate dehydrogenase (positive control).

GDD1 gene expression during myogenesis and osteogenesis

There is considerable interest in the mechanisms of development and differentiation of skeletal muscles and bone tissues. A murine pluripotent mesenchymal precursor cell line, C2C12, has been proven to be a good in vitro model for myogenic and osteoblastic differentiation [13]. When cultured in low-serum-containing medium (Myogenic DM), C2C12 cells form readily apparent multinucleated myotubes by day 3. On the other hand, stimulation with bone morphogenetic protein 2 (BMP-2) not only blocks myogenic differentiation of C2C12 cells but also induces osteoblast differentiation. Since our Northern blot analysis showed high *GDD1* expression in skeletal muscle and bone, we tested whether myogenic or osteoblastic induction in C2C12 cells alters *GDD1* expression. Inductions of myogenesis and osteogenesis were confirmed both morphologically (data not shown) and by the expressions of differentiation markers, troponin T (TnT; muscle differentiation marker) and osteocalcin (OC; differentiated osteoblast marker) genes (Fig. 3). While we observed relatively low *GDD1* expression in undifferentiated C2C12 cells, *GDD1* expression was up-regulated during the course of myogenic differentiation, in parallel with expression of the troponin T gene.

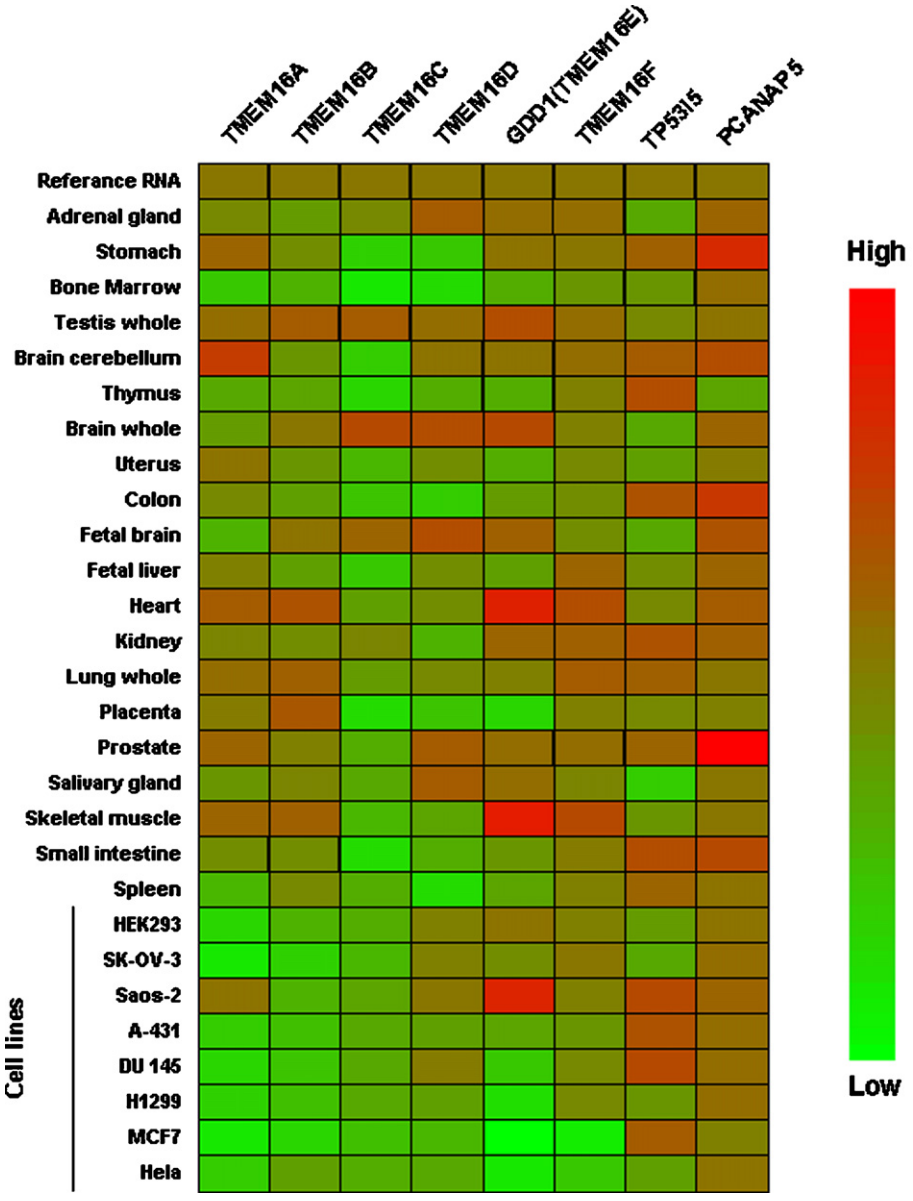

Fig. 4. Expression analysis of the human *GDD1*-related gene family (TMEM16 gene family). Expression levels of each TMEM16 gene were analyzed by real-time PCR using TaqMan probes and normalized with the level of *β-actin* expression. TaqMan assay IDs were described in Materials and methods. The red-green pseudocolor chart depicts TMEM16 gene expression data and allows comparisons among 20 different tissues and eight cell lines. Red blocks depict tissues or cell lines that are relatively over-expressed in comparison to a reference sample (Top blocks, the Universal Human Reference Total RNA, BD Biosciences), whereas green blocks depict tissues or cell lines that are relatively under-expressed.

In contrast, *GDD1* expression was diminished during osteoblastic differentiation. While the biological significance of this observation remains to be determined, given the abundant *GDD1* expression in adult skeletal muscle, GDD1 may play essential roles in controlling myoblast proliferation and differentiation. To test this hypothesis, experiments designed to determine whether constitutive over-expression of exogenous *GDD1* in C2C12 or siRNA-mediated gene silencing can affect the myogenic differentiation process are underway in our laboratory.

Expression analysis of human GDD1-related genes (TMEM16 family)

Recently, on the basis of sequence conservation and the computational similarities of predicted secondary protein structures, Katoh et al. [7–11] proposed a previously uncharacterized novel gene family termed TMEM16. The human TMEM16 family has at least eight members including GDD1: ORAOV2 (TMEM16A), TMEM16B, TMEM16C, TMEM16D, GDD1 (TMEM16E, LOC203859), DKFZp313M0720 (TMEM16F), TP53I5 (PIG5), and PCANAP5 (NGEP). Like *GDD1* gene, members of the TMEM16 family are predicted to encode mutually homologous proteins containing eight-transmembrane domains, with the N- and C-terminal tails facing the cytoplasm. Interestingly, the TMEM16 family shares the conserved sequence motif DUF590, which mapped to approximately the third intracellular loop of the TMEM16 proteins. It is likely that GDD1 and other members of this family have, at a minimum, similar cellular functions and display similar cellular localization patterns. Therefore, discovering the functions of other members of the TMEM16 may facilitate elucidating GDD1 function. Unfortunately, none of the TMEM16 proteins have as yet been well characterized, and only a few have been experimentally verified. We therefore analyzed the expressions of human TMEM16 members in various human tissues and cell lines by quantitative real-time RT-PCR analysis. Results are shown in Fig. 4 using a red-green color scale. Expression patterns of human *GDD1* mRNA were consistent with our previous observations [6], with high levels of expression detected in heart and skeletal muscle. Among cell lines, *GDD1* expression was detected at a significant level only in Saos-2 cells, a human osteosarcoma cell line. Expressions of TMEM16A, TMEM16B, and TMEM16F mRNA largely overlapped with that of *GDD1* mRNA but exhibited a more ubiquitous pattern. TMEM16A was most abundant in the cerebellum. TMEM16C expression was largely restricted to testis and brain. Expression levels for TMEM16B and TMEM16C were low in cell lines, as compared to those in tissues. High levels of TP53I5 expression were detected in the thymus, gastro-intestinal tracts (stomach, small intestine, and colon), and several carcinoma derived cell lines, such as A-431, DU 145, and MCF7. PCANAP5 mRNA was most abundantly expressed in the prostate, and significant expression was also observed in other tissues including the gastro-intestinal tracts. The PCANAP5 (NGEP) gene was previously reported to be expressed specifically in both normal prostate and the prostate cancer [12].

Conclusion and implications

In this study, we have characterized the mouse counterpart of human *GDD1* mRNA. Based on its gene structure, we are currently adopting the strategy of generating *GDD1* knockout mice to investigate the in vivo function of the product of this gene. Multiple alternative splicing events with putative changes in GDD1 functions and structural topologies suggested diverse cellular roles of GDD1 protein. *GDD1* expression was up-regulated during in vitro myogenic cell differentiation, suggesting important roles in myoblast proliferation and differentiation. Finally, an extensive expression profile of human *GDD1*-related TMEM16 genes may facilitate elucidating the functions of each gene and also to discover human diseases associated with TMEM16 gene mutations other than GDD/*GDD1*.

Acknowledgments

This work was supported by grants from the Takeda Science Foundation for Bioscience and the Uehara Memorial Foundation (S.T.), and the Grant-in-Aid from the Japan Society for Promoting Science (N.K., No. 16659555). H.I. gratefully acknowledges support from the Mitsubishi Foundation.

References

[1] Y. Akasaka, T. Nakajima, K. Koyama, K. Furuya, Y. Mitsuka, Familial cases of new systemic bone disease, hereditary gnathodiaphyseal sclerosis, Nippon Seikeigeka Gakkai Zasshi 43 (1969) 381–394.

[2] M. Riminucci, M.T. Collins, A. Corsi, A. Boyde, M.D. Murphey, S. Wientroub, S.A. Kuznetsov, N. Cherman, P.G. Robey, P. Bianco, Gnathodiaphyseal dysplasia: a syndrome of fibro-osseous lesions of jawbones, bone fragility, and long bone bowing, J. Bone Miner. Res. 16 (2001) 1710–1718.

[3] L.S. Levin, J.M. Wright, D.L. Byrd, G. Greenway, J.P. Dorst, R.N. Irani, R.E. Pyeritz, R.J. Young, C.L. Laspia, Osteogenesis imperfecta with unusual skeletal lesions: report of three families, Am. J. Med. Genet. 21 (1985) 257–269.

[4] A. Toffanin, R. Benetti, R. Manconi, Familial florid cemento-osseous dysplasia: a case report, J. Oral Maxillofac. Surg. 58 (2000) 1440–1446.

[5] S. Tsutsumi, N. Kamata, Y. Maruoka, M. Ando, O. Tezuka, S. Enomoto, K. Omura, M. Nagayama, E. Kudo, M. Moritani, T. Yamaoka, M. Itakura, Autosomal dominant gnathodiaphyseal dysplasia maps to chromosome 11p14.3–15.1, J. Bone Miner. Res. 18 (2003) 413–418.

[6] S. Tsutsumi, N. Kamata, T.J. Vokes, Y. Maruoka, K. Nakakuki, S. Enomoto, K. Omura, T. Amagasa, M. Nagayama, F. Saito-Ohara, J. Inazawa, M. Moritani, T. Yamaoka, H. Inoue, M. Itakura, The novel gene encoding a putative transmembrane protein is mutated in gnathodiaphyseal dysplasia (GDD), Am. J. Hum. Genet. 74 (2004) 1255–1261.
[7] M. Katoh, M. Katoh, FLJ10261 gene, located within the CCND1-EMS1 locus on human chromosome 11q13, encodes the eight-transmembrane protein homologous to C12orf3, C11orf25 and FLJ34272 gene products, Int. J. Oncol. 22 (2003) 1375–1381.
[8] M. Katoh, M. Katoh, Identification and characterization of TMEM16E and TMEM16F genes in silico, Int. J. Oncol. 24 (2004) 1345–1349.
[9] M. Katoh, M. Katoh, Identification and characterization of human TP53I5 and mouse Tp53i5 genes in silico, Int. J. Oncol. 25 (2004) 225–230.
[10] M. Katoh, M. Katoh, Characterization of human TMEM16G gene in silico, Int. J. Mol. Med. 14 (2004) 759–764.
[11] M. Katoh, M. Katoh, GDD1 is identical to TMEM16E, a member of the TMEM16 family, Am. J. Hum. Genet. 75 (2004) 927–928.
[12] T.K. Bera, S. Das, H. Maeda, R. Beers, C.D. Wolfgang, V. Kumar, Y. Hahn, B. Lee, I. Pastan, NGEP, a gene encoding a membrane protein detected only in prostate cancer and normal prostate, Proc. Natl. Acad. Sci. USA 101 (2004) 3059–3064.
[13] T. Katagiri, A. Yamaguchi, M. Komaki, E. Abe, N. Takahashi, T. Ikeda, V. Rosen, J.M. Wozney, A. Fujisawa-Sehara, T. Suda, Bone morphogenetic protein-2 converts the differentiation pathway of C2C12 myoblasts into the osteoblast lineage, J. Cell Biol. 127 (1994) 1755–1766.
[14] A. Oren, A. Toporik, S. Biton, N. Almogy, D. Eshel, J. Bernstein, K. Savitsky, G. Rotman, hCHL2, a novel chordin-related gene, displays differential expression and complex alternative splicing in human tissues and during myoblast and osteoblast maturation, Gene 331 (2004) 17–31.